AMERICAN SOCIETY FOR MICROBIOLOGY | Journal of Virology

Editor's Pick | Molecular and Cellular Biology | Full-Length Text

Ectopic expression of murine CD163 enables cell-culture isolation of lactate dehydrogenase-elevating virus 63 years after its discovery

Teressa M. Shaw,[1] Sara M. Maloney,[1] Kylie Nennig,[1] Mitchell D. Ramuta,[1] Andrew Norton,[1] Rodrigo Ibarra,[1] Paul Kuehnert,[1] Margo Brinton,[2] Kay Faaberg,[3] Jens H. Kuhn,[4] David H. O'Connor,[1] Cody J. Warren,[5] Adam L. Bailey[1]

AUTHOR AFFILIATIONS See affiliation list on p. 14.

ABSTRACT Arteriviruses are RNA viruses related to coronaviruses but have not yet been associated with human infection. A murine arterivirus, lactate dehydrogenase-elevating virus (LDV), was first described in 1960 and quickly became a promising model for understanding immune failure due to its unique ability to persist in immunocompetent adult mice. However, the inability to culture LDV *in vitro* ultimately limited this system. Here, we demonstrate that the macrophage marker CD163 is essential for LDV infection. Expression of the murine homolog (mCD163) in otherwise mCD163-negative cell lines from mice and nonhuman primates enables productive LDV infection, creating the first immortalized cell-culture system. We also show that mCD163-knockout mice are completely resistant to LDV infection. These findings advance LDV as a model of arterivirus infection and viral persistence while adding to a growing body of literature suggesting that CD163 utilization is a broad feature of arteriviruses.

IMPORTANCE Mouse models of viral infection play an especially large role in virology. In 1960, a mouse virus, lactate dehydrogenase-elevating virus (LDV), was discovered and found to have the peculiar ability to evade clearance by the immune system, enabling it to persistently infect an individual mouse for its entire lifespan without causing overt disease. However, researchers were unable to grow LDV in culture, ultimately resulting in the demise of this system as a model of failed immunity. We solve this problem by identifying the cell-surface molecule CD163 as the critical missing component in cell-culture systems, enabling the growth of LDV in immortalized cell lines for the first time. This advance creates abundant opportunities for further characterizing LDV in order to study both failed immunity and the family of viruses to which LDV belongs, *Arteriviridae* (aka, arteriviruses).

KEYWORDS lactate dehydrogenase-elevating virus, arterivirus, CD163, porcine reproductive and respiratory syndrome virus, simian hemorrhagic fever virus, PRRSV, SHFV

Arteriviruses (*Nidovirales: Arteriviridae*) are positive-sense RNA viruses that produce enveloped particles (1, 2). Distinct arteriviruses have been discovered in metatherians (possums) and eutherians (hedgehogs, horses, monkeys, rodents, pigs, and shrews), suggesting a vast natural diversity of these viruses, with host-versus-virus phylogenetic comparisons revealing multiple cross-species transmission events (3–5). Five archetypal mammalian arteriviruses have been studied in the laboratory: equine arteritis virus (EAV), lactate dehydrogenase-elevating virus (LDV) of mice, simian hemorrhagic fever virus (SHFV), and porcine reproductive and respiratory syndrome viruses 1 and 2 (PRRSV-1/2). These viruses can evade and antagonize host immune responses enabling

Editor Tom Gallagher, Loyola University Chicago, Maywood, Illinois, USA

Address correspondence to Adam L. Bailey, albailey@wisc.edu.

Teressa M. Shaw, Sara M. Maloney, and Kylie Nennig contributed equally to this article. Author order was determined by project leadership and agreed to by all authors.

The authors declare no conflict of interest.

See the funding table on p. 14.

Received 29 June 2023
Accepted 8 August 2023
Published 4 October 2023

them to persist subclinically, often for the lifespans of the hosts. However, in a subset of individuals (e.g., newborns or non-natural hosts), arteriviruses can cause a range of diseases, including arteritides, spontaneous abortions, pneumonias, encephalitides, and hemorrhagic fevers (2).

LDV was first described in 1960 as a "transmissible enzymic lesion" that could be identified by an increase in serum lactate dehydrogenase activity in infected laboratory mice with experimental tumors (6). Despite being a lytic virus, LDV persists for the lifespan of the mouse—a rare feature among RNA viruses that resulted in its development as a tool to interrogate mechanisms of failed immunity (7, 8). LDV infection robustly induces classic effectors of antiviral immunity (e.g., cytokines, antibodies, and cytotoxic T cells). However, these responses are incapable of exerting more than a modest antiviral effect on LDV replication and viremia (7). How LDV is capable of persisting in the presence of these immune responses remains largely unknown (7). The primary target of LDV infection appears to be a poorly defined yet renewable subpopulation of macrophages within the peritoneum, spleen, liver, and bone marrow (7, 9, 10). Indeed, primary peritoneal macrophages can be productively infected with LDV *ex vivo* (11). Immortalized cell lines do not consistently support LDV replication but can produce infectious virus particles upon transfection of LDV genomic RNA, suggesting the absence of a critical receptor or host factor involved in virion entry (7, 12–14). The lack of reliable *in vitro* systems and increasingly sophisticated systems for manipulating lymphocytic choriomeningitis virus (LCMV; *Bunyavirales: Arenaviridae*), another semi-persistent virus of house and laboratory mice, ultimately led to the demise of LDV infection as a viral immunology model.

Arteriviruses in general appear to be highly restricted in cell tropism. LDV is unable to replicate in immortalized cell lines, and PRRSV-1/2 and SHFV, for instance, can be propagated only in a very limited set of immortalized cell lines (e.g., MA-104 and its derivatives) (1). Thus, a conundrum exists in arterivirus research: LDV cannot be studied easily *in vitro*, and *in vivo* studies of other arteriviruses can only be performed in large and relatively intractable animal systems (e.g., horses, pigs, or monkeys).

The 3′ half of the arterivirus genome contains 8–12 overlapping open reading frames (ORFs) that are expressed as a nested set of subgenomic RNAs that serve as templates for mRNA synthesis (1, 2). Many of these ORF products are inserted and/or protrude from the arterivirion membrane, resulting in an unusually large number of virion surface proteins available for multivalent interactions with host attachment factors and receptors (15, 16). The large number of surface proteins, their relatively small ectodomains available for antibody recognition, and the high degree of ectodomain glycosylation may all be contributing factors in LDV's persistence (7).

The unique features of the arterivirion surface proteins have also hindered identification of bona fide arterivirus receptors, although several have been proposed. Of these, only porcine CD163, the cell-surface hemoglobin:haptoglobin scavenger receptor that also serves as a specific marker for tissue-resident macrophages, has been determined to be essential for PRRSV-1/2 infection *in vivo* (17, 18).

We recently demonstrated that primate CD163 orthologs enable SHFV infection of multiple cell lines (19), suggesting that CD163 utilization may be a broader feature of arterivirus biology than previously recognized. Consequently, we hypothesized that murine CD163 (mCD163) is the receptor for LDV and could be the missing critical host factor required for LDV growth in cell culture.

RESULTS

Murine myeloid cell lines resistant to LDV infection do not express mCD163

Using the well-characterized Plagemann strain of LDV (LDVp) (7), we first created a virus stock and quantified viral RNA using LDVp-specific real-time reverse transcription polymerase chain reaction (RT-qPCR); the copy number for the nucleocapsid (*N*) gene was determined using a synthetic RNA standard curve. Next, we performed a 24-h growth curve on primary cells collected via peritoneal lavage (i.e., peritoneal

macrophages)—commonly used for propagating LDV *ex vivo* (11, 20)—and several immortalized cell lines (house mouse RAW 264.7 macrophages, laboratory mouse ImKC Kupffer cells, laboratory mouse BV-2 microglia, house mouse J774A.1 macrophages, and laboratory mouse NIH/3T3 fibroblasts). Cells were inoculated, and LDVp RNA was extracted from supernatants and quantified by RT-qPCR. As expected, primary peritoneal cells supported robust LDVp replication, whereas immortalized cell lines did not (Fig. 1a). Using RT-qPCR with mCD163 gene-specific primers, we readily detected mCD163 mRNA in primary peritoneal lavage cells but failed to detect mCD163 mRNA in any of the immortalized cell lines (Fig. 1b).

Ectopic expression of mCD163 renders multiple murine cells susceptible to LDV

Using RNA extracted from laboratory mouse peritoneal monocytes and macrophages, we cloned cDNA encoding mCD163 transcript variant 1 (gene ID: 93671) into multiple systems for stable expression. Introduction of these mCD163 constructs into immortalized murine cell lines resulted in mCD163 expression, as detected by flow cytometry (Fig. 2a; Fig. S1). Upon inoculation with LDVp, all mCD163$^+$ cell lines (except BV-2) produced detectable LDVp RNA in the culture supernatants over time (Fig. 2b). NIH/3T3 + mCD163 cells were unique in their ability to form adherent monolayers and develop substantial cytopathic effects (Fig. S2), making them an obvious choice for plaque assay development. Inoculation with LDVp, followed by methylcellulose overlay, indeed resulted in visible plaques (Fig. 2c). Together, these data indicate that mCD163 is a necessary factor required for production of infectious LDVp.

Divergent LDV strains require mCD163 for infection

LDVp is a distinct LDV strain that is highly resistant to antibody neutralization *in vivo* (21, 22). To determine whether other strains of LDV also required mCD163 for infection, we acquired LDV C strain (LDVc), which, in contrast to LDVp, is highly immunogenic (23–25). We also obtained a previously uncharacterized LDV strain from a wild house

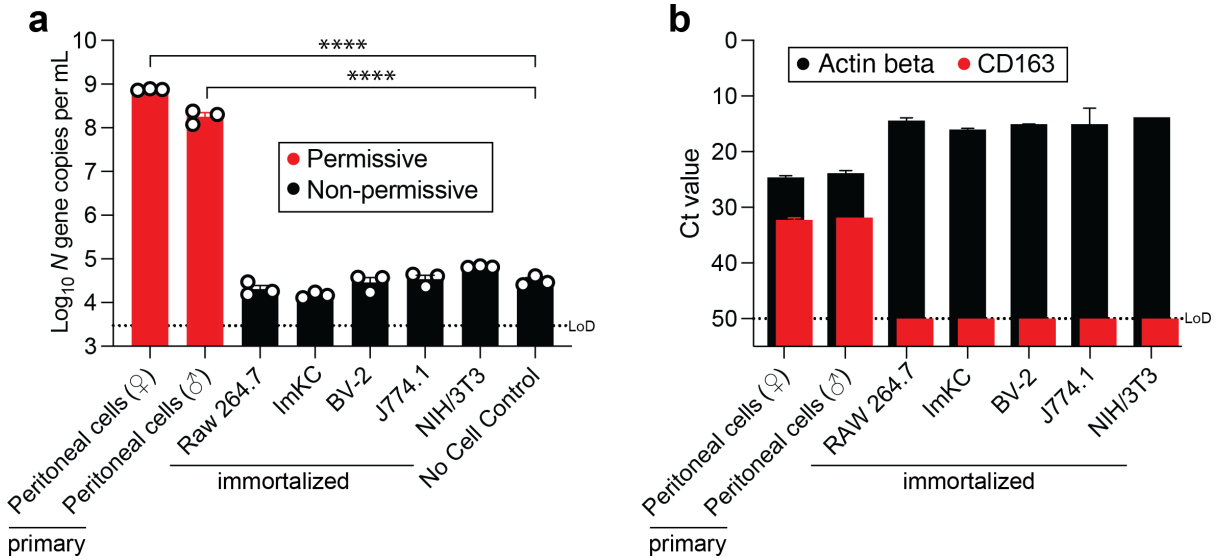

FIG 1 Murine myeloid cell lines resistant to LDV infection do not express mCD163. (a) LDVp replication in murine cells. Cells collected from laboratory mice by peritoneal lavage (pastel red) or immortalized murine cell lines (black) were inoculated with an MOI of 0.07 LDVp *N* gene copies per cell. LDVp RNA in the supernatant was quantified by LDVp-specific RT-qPCR after 24 h. Error bars show the standard error of the mean (SEM). Statistical significance was determined using one-way analysis of variance (ANOVA) with a no-cell control as a reference, with **** representing $P < 0.0001$. (b) mCD163 expression in murine cells. RNA was extracted from 2.5×10^5 to 1×10^6 cells and subjected to RT-qPCR to detect mCD163 (pastel red) or actin beta (black) or mRNA. Ct, cycle threshold; LDVp, lactate dehydrogenase-elevating virus Plagemann strain; LoD, limit of detection; mCD163, murine CD163 molecule; MOI, multiplicity of infection; *N*, nucleocapsid gene RT-qPCR, real-time reverse transcription polymerase chain reaction. Graphs show one of two independent repeats.

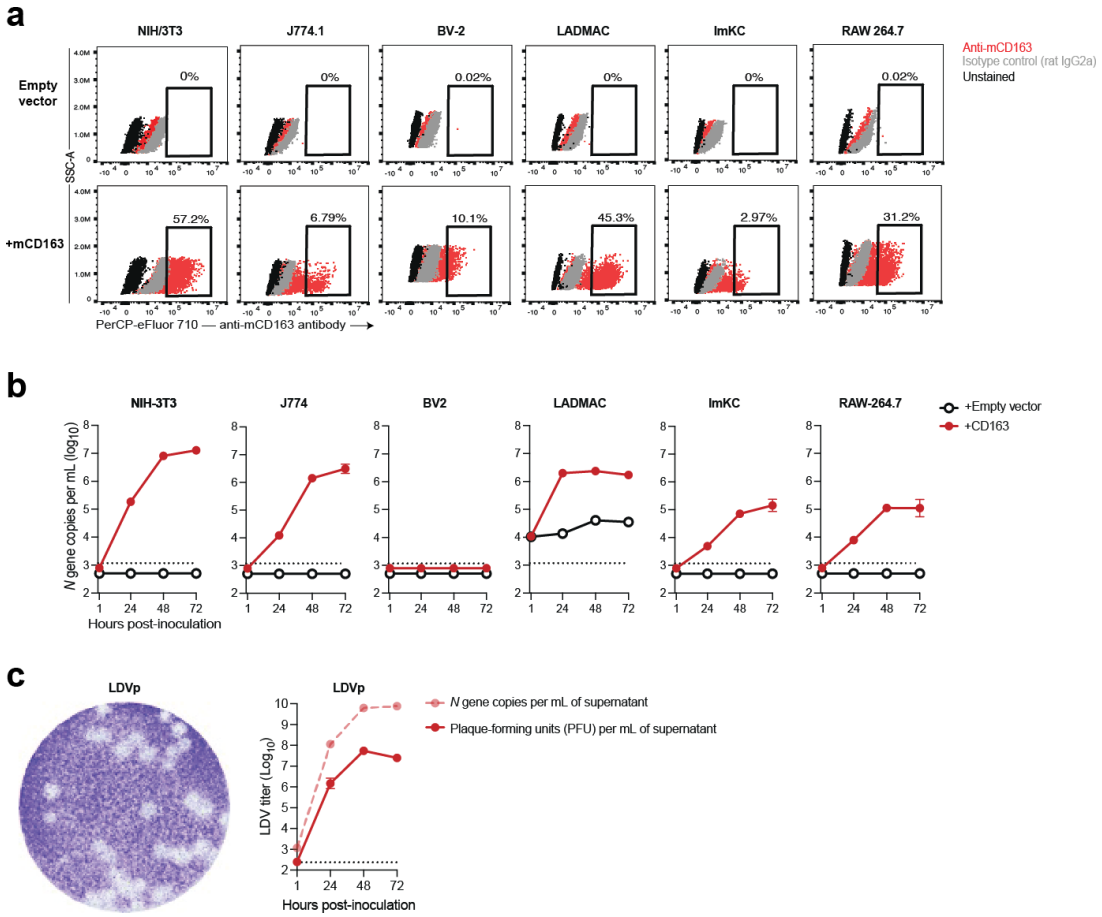

FIG 2 Ectopic expression of mCD163 renders multiple murine cells susceptible to LDV. (a) Expression of mCD163 in murine cells. Flow cytometry dot plots of murine cell lines transduced with empty vector (top) or mCD163-expressing (bottom) retroviruses and stained with anti-mCD163 antibody (red), isotype control antibody (gray), or unstained (black) after fixation and permeabilization. (b) LDVp replication in murine cell lines ectopically expressing mCD163. Inoculation of the same cell lines shown in panel a (empty vector, black with open circles; +mCD163, red with solid circles) with LDVp (MOI = 0.07 *N* gene copies per cell). After 1 h, inocula were removed (except for LADMAC because it is a suspension cell line), cells were washed, and supernatants were collected at 1, 24, 48, and 72 h post-inoculation. LDV RNA was quantified by RT-qPCR (n = 3 per group). Error bars show the standard error of the mean (SEM). (c) Plaque formation by LDVp in NIH/3T3 + mCD163 fibroblasts. Plaque assay for LDVp using a confluent monolayer of NIH/3T3 + mCD163 cells. A time course of LDVp (MOI 0.01 PFU) shows the production of LDVp RNA (measured by *N* gene copies; dashed line) vs LDVp (measured by PFU; solid line) over time (n = 3 per group). IgG, immunoglobulin G; LDVp, lactate dehydrogenase-elevating virus Plagemann strain; mCD163, murine CD163 molecule; MOI, multiplicity of infection; *N*, nucleocapsid gene; PFU, plaque-forming units; RT-qPCR, real-time reverse transcription polymerase chain reaction. Graphs show one of two independent repeats.

mouse, which we termed LDVw. Viruses were propagated by intraperitoneal inoculation of laboratory mice, and stocks were made by bleeding mice at 24 h post-inoculation and diluting serum in phosphate-buffered saline (PBS). Deep sequencing of LDV stocks revealed many consensus-level differences between published LDV sequences (24, 26) and our LDV stocks (Fig. 3a). Phylogenetic comparisons with other arteriviruses showed that LDVp, LDVc, and LDVw form a monophyletic clade, with LDVw most closely related to LDVp (Fig. 3a and b), sharing 86.8% nucleotide identity. LDVc is more divergent, sharing 78.5% and 77.6% nucleotide identity with LDVp and LDVw, respectively. Differences among these three LDV strains are spread unevenly across the genome, with the *N* gene being most highly conserved. The greatest divergence was seen in polyprotein 1a and regions in which ORFs overlapped (Fig. 3c). Despite these differences, all LDV strains productively infected NIH/3T3 fibroblasts expressing mCD163 but did not infect NIH/3T3 empty-vector cells (Fig. 3d and e).

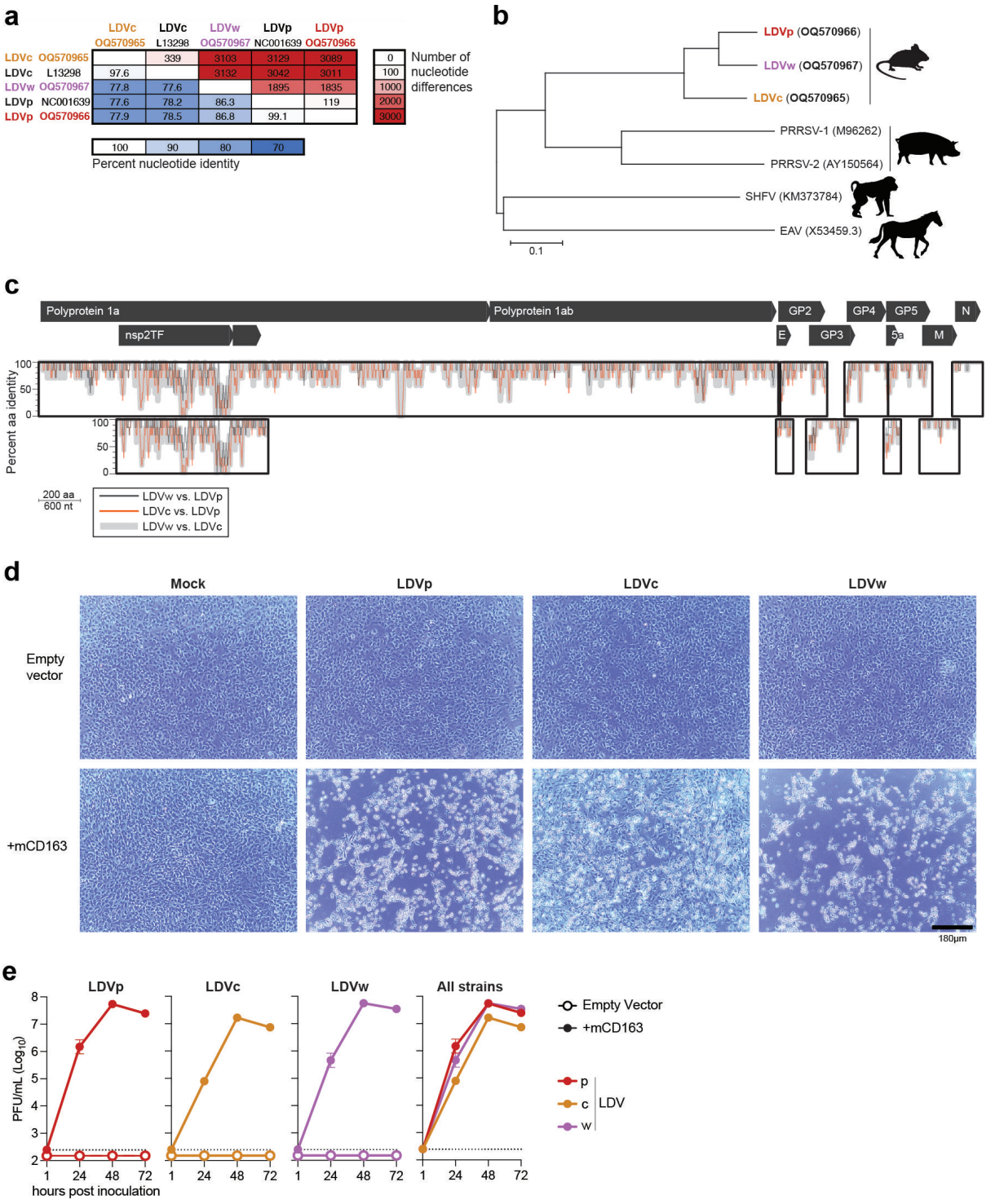

FIG 3 Divergent LDV strains require mCD163 for infection. LDV strains were propagated once in laboratory mice and then analyzed by deep sequencing. (a) Comparison of coding-complete LDV strain genome sequences obtained during this study (ochre, purple, red) with previously reported sequences (black). Percent identities are shown in the lower left of the table, with increasing sequence divergence heat mapped toward darker shades of blue. Numbers of nucleotide differences between each coding-complete genome are shown in the upper right of the table, with increasing sequence divergence heat mapped toward darker shades of red. (b) Phylogeny based on the coding-complete genomes of the archetypal arteriviruses (GenBank accession number in parentheses), including LDV strains used in this study (colored as in panel a). The tree is drawn to scale, with branch lengths measured in the number of substitutions per site (scalebar). Bootstrap support is 100% support for each node. (c) Schematic of the ORFs spanning the LDV genome, with simplot analyses comparing amino acid changes corresponding to the proteins encoded by each ORF displayed for LDVp, LDVc, and LDVw underneath. (d) CPE of divergent LDV strains

(Continued on next page)

FIG 3 (Continued)

on NIH/3T3 + mCD163 or mock-transfected cells at 3 d post-inoculation with an MOI = 0.01. (e) Plaque titration of LDV strain production in supernatants of NIH/3T3 + empty vector cells (open circles) and NIH/3T3 + mCD163 cells (solid circles) over time (n = 3 per group). Error bars show the standard error of the mean (SEM). Sequencing and plaque time-course experiments were performed once. CPE, cytopathic effect; E, envelope protein EAV, equine arteritis virus; GP, glycoprotein; LDV, lactate dehydrogenase-elevating virus; LDVc, LDV C strain; LDVp, LDV Plagemann strain; LDVw, LDV wild house mouse strain; M, membrane protein mCD163, murine CD163 molecule; MOI, multiplicity of infection; N, nucleocapsid protein PRRSV, porcine reproductive and respiratory syndrome virus; SHFV, simian hemorrhagic fever virus.

Ectopic expression of mCD163 renders grivet cells permissive to LDV infection

PRRSV-1/2 and SHFV productively infect embryonic grivet MA-104 kidney cells, but LDV does not. We hypothesized that this discrepancy could be due to subtle difference among CD163 orthologs and thus expressed mCD163 in MA-104 cells (Fig. 4a; Fig. S3). Indeed, MA-104 + mCD163 cells produced infectious LDV after inoculation with any of the three LDV strains, as determined by plaque assay (Fig. 4a through d; Fig. S4), and cytopathic effect was observed. Given the propensity for NIH/3T3 fibroblasts to spontaneously differentiate into adipocyte-like cells upon reaching confluency (27), MA-104 + mCD163 cells likely represent a more stable and reproducible cell line for future *in vitro* work with LDV and related arteriviruses.

CD163 is required for LDV infection in laboratory mice

To examine the importance of CD163 for LDV infection in primary cells, we obtained homozygous mCD163-knockout (*mCD163*$^{-/-}$) mice. As expected, cells sampled via peritoneal lavage from m*CD163*$^{-/-}$ mice did not express mCD163, whereas ≈3% of cells from wild-type mice were positive for mCD163 expression by flow cytometry (Fig. 5a; Fig. S5). Peritoneal lavage cell cultures from wild-type mice supported robust LDVp replication, but peritoneal lavage cell cultures from *mCD163*$^{-/-}$ mice did not (Fig. 5b). To extend these findings, wild-type (*mCD163*$^{+/+}$), heterozygous mCD163-knockout (*mCD163*$^{+/-}$), and *mCD163*$^{-/-}$ littermates were intraperitoneally injected with LDVp. Heterozygous mCD163 expression had no effect on LDVp viremia compared to wild-type homozygous CD163 expression, as determined by LDVp-specific RT-qPCR. However, homozygous *mCD163*$^{-/-}$ mice had significantly lower viral loads at 1 d post-inoculation and undetectable LDVp RNA in sera by 15 d post-inoculation (Fig. 5c). To broaden these findings to the other LDV strains, we inoculated *mCD163*$^{-/-}$ mice with LDVp, LDVc, or LDVw and measured viral loads by plaque assay. Viremia was not detectable at any timepoint in LDV-inoculated *mCD163*$^{-/-}$ mice, whereas inoculation of wild-type mice resulted in high-titer viremia (Fig. 5d). To further examine the extent to which LDV relies on mCD163 for infection *in vivo*, we performed *in situ* hybridization using samples of spleens—a well-described site of acute-phase LDVp replication (9)—collected from wild-type and *CD163*$^{-/-}$ mice at 1 d post-inoculation. Splenic tissues from wild-type mice revealed robust staining of LDVp RNA that localized to the white pulp; however, LDVp RNA staining in splenic tissues from *CD163*$^{-/-}$ mice was similar to LDVp staining in spleens from LDV-unexposed wild-type mice (Fig. 5e).

DISCUSSION

Mouse models are essential for understanding how the immune system responds to viral infection. In the 1960s, LDV was discovered; its ability to persist in the blood of mice indefinitely held great promise for interrogating immune function and mechanisms of immune failure. However, unlike other model viruses (or other arteriviruses), LDV would not replicate in immortalized cell lines, ultimately limiting its utility. In this study, we showed that mCD163—a host molecule with expression restricted to the known LDV target cell (macrophages)—is required for LDV infection and is notably absent on immortalized murine macrophage cell lines. Introduction of mCD163 into various cell lines enabled growth of LDV in immortalized cells, and knockout of mCD163 in

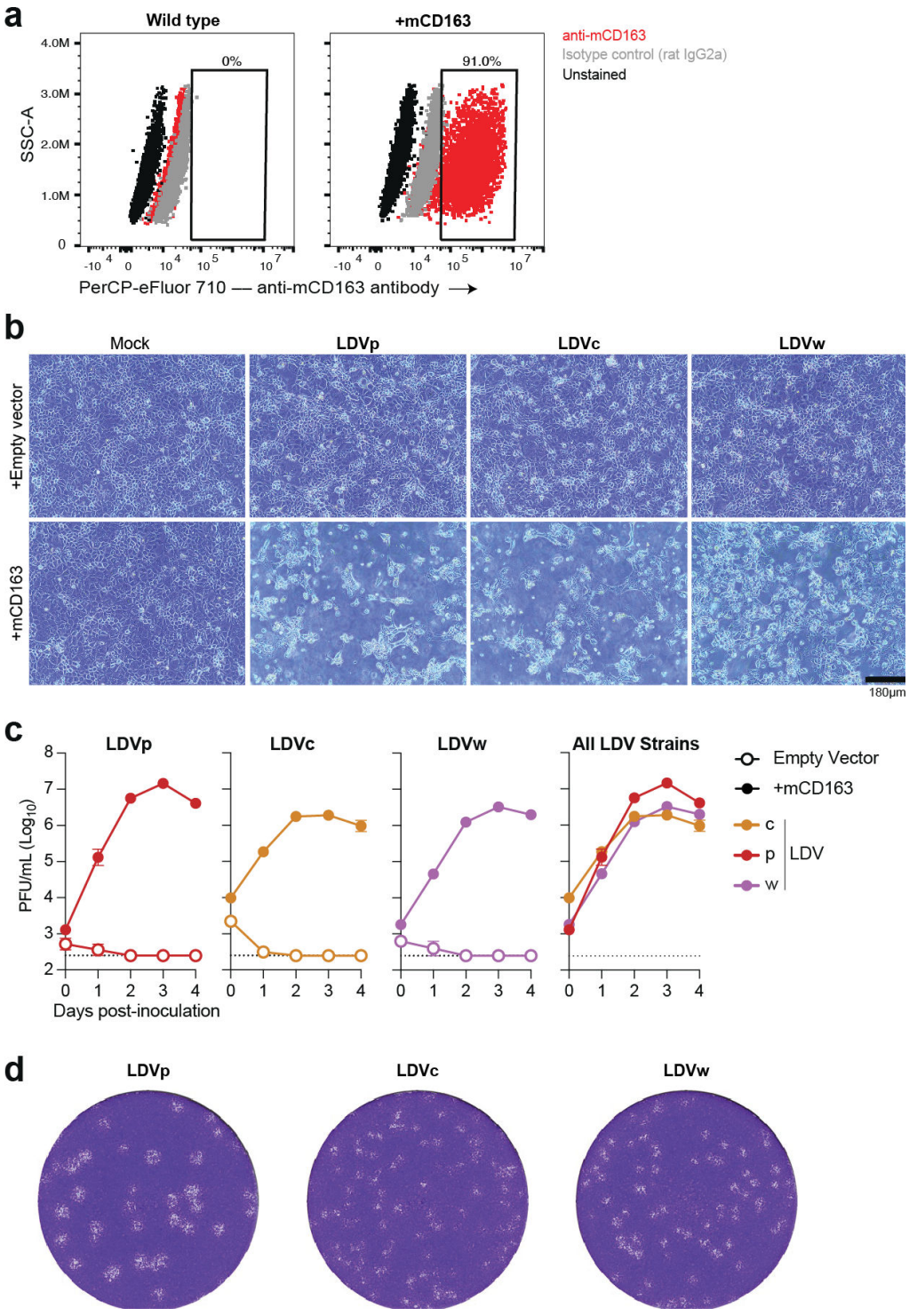

FIG 4 Ectopic expression of mCD163 renders grivet cells permissive to LDV infection. (a) Quantification of mCD163 in MA-104 cells by flow cytometry after fixation and permeabilization. (b) Representative photos of CPE of MA-104 cells inoculated with LDV strains at an MOI of 0.01 taken 4 d post-inoculation. (c) Plaque titration of LDV strain production in supernatants of MA-104 + empty vector cells (open circles) and MA-104 + mCD163 cells (solid circles) over time (n = 3 per group). Error bars show the standard error of the mean (SEM). (d) Plaque assays on MA-104 + mCD163. Experiments were performed once. CPE, cytopathic effect; IgG, immunoglobulin G; LDV, lactate dehydrogenase-elevating virus; LDVc, LDV C strain; LDVp, LDV Plagemann strain; LDVw, LDV, wild house mouse strain; mCD163, murine CD163 molecule; MOI, multiplicity of infection.

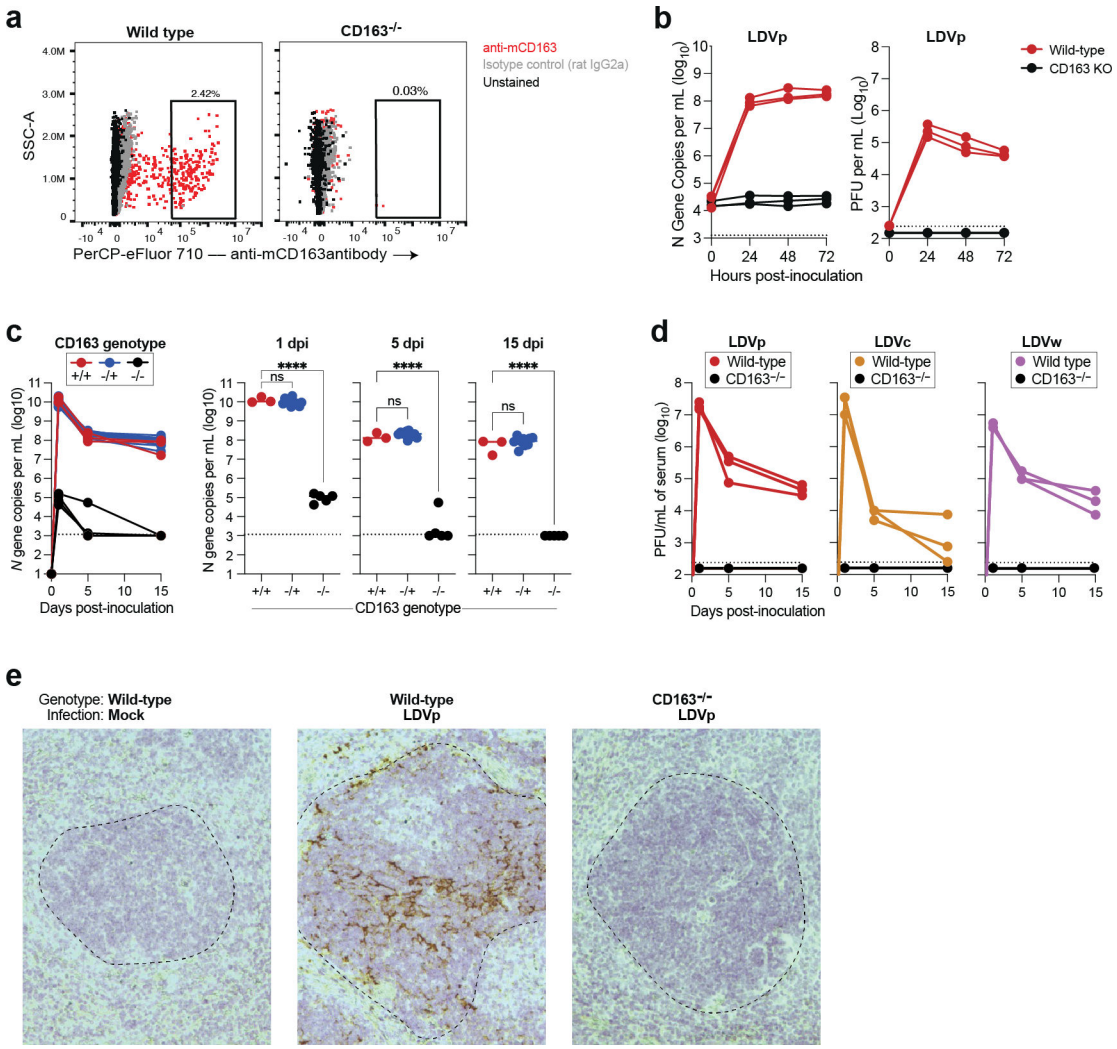

FIG 5 CD163 is required for LDV infection in laboratory mice. (a) mCD163 expression in laboratory mouse peritoneal cells. Flow cytometry dot plots of freshly collected peritoneal cells from wild-type (left) or mCD163$^{-/-}$ (right) mice stained with anti-mCD163 antibody (red), isotype control antibody (gray), or unstained (black) after fixation and permeabilization. (b) LDVp replication in mouse peritoneal cells. Production of LDVp RNA (left) or formation of plaque-forming units (right) in wild-type (red [top plot lines]) and mCD163$^{-/-}$ (black [bottom plot lines]) mice over time (n = 3 per group). (c) LDV viremia in wild-type (mCD163$^{+/+}$, red, n = 3), heterozygous mCD163-knockout (mCD163$^{+/-}$, blue, n = 11), and homozygous mCD163-knockout (mCD163$^{-/-}$, black [bottom plot lines], n = 5) littermates inoculated intraperitoneally with 7 × 10^6 N gene copies of LDVp. Serum viral loads were quantified using LDVp-specific RT-qPCR at 1, 5, and 15 d post-inoculation. Statistical significance was determined using one-way analysis of variance (ANOVA) with wild type as the reference, with **** representing P < 0.0001. (d) mCD163$^{+/+}$ [colored (top plot lines)] and homozygous mCD163$^{-/-}$ [black (bottom plot lines)] mice were inoculated intraperitoneally with 1 × 10^4 PFU/mL of LDVp, LDVc, or LDVw (n = 3 per group), and serum viral loads were quantified by plaque assay on MA-104 + mCD163 cells at 1, 5, and 15 d post-inoculation. (e) Representative staining of LDV RNA in the spleens of unexposed wild-type mice (left), LDV-inoculated wild-type mice (middle), and LDV-inoculated mCD163$^{-/-}$ mice (right) at 1 d post-exposure using LDV-specific *in situ* hybridization (brown) counterstained with Gill's hematoxylin. The dashed line demarcates the red pulp (lighter staining tissue) from the white pulp (stained blue). Experiments were performed once. dpi, day post-inoculation; IgG, immunoglobulin G; LDV, lactate dehydrogenase-elevating virus; LDVc, LDV C strain; LDVp, LDV Plagemann strain; LDVw, LDV, wild house mouse strain; mCD163, murine CD163 molecule; PFU, plaque-forming units; RT-qPCR, real-time reverse transcription polymerase chain reaction.

laboratory mice rendered them completely resistant to LDV infection. Our discovery of mCD163 as the putative receptor for LDV has enabled the creation of systems for culturing LDV in immortalized cell lines. With this advance, we have created a tractable, small-animal laboratory system for studying arterivirus biology both *in vitro* and *in vivo*. The mouse as a host for this "complete set" of tools creates abundant opportunities to

leverage the extensive suite of murine reagents and transgenic systems to study LDV for the advancement of several scientific objectives.

First, this discovery should reposition LDV as a model of viral persistence and immune failure. The successful use of LCMV as an immunological tool provides a blueprint for advancing the LDV model within this objective. Given the likely differences in persistence mechanisms between LCMV and LDV, we anticipate that further defining the mechanisms of immune failure and persistence in LDV infection will provide unique insights into immune function. Although persistent RNA viruses have long been a bane to human health (e.g., human immunodeficiency viruses, human T cell lymphotropic viruses, and hepatitis C virus), the ability of "acute" viruses to persistently infect some individuals (i.e., Ebola virus and SARS-CoV-2)—with significant implications for viral pathogenesis, immunopathogenesis, and disease transmission—highlights the urgent need for new insights into mechanisms of immune failure against viruses. Given the critical role of laboratory mice in immunology research, it seems plausible that the LDV model may be leveraged in parallel with LCMV to draw more generalizable knowledge out of immunology studies using models of viral persistence.

Second, the advancement of the LDV model also has implications for defining host barriers to viral infection. *Arteriviridae* is the only family of mammalian RNA viruses that does not have members known to infect humans (28). However, several features of arteriviruses—their vast genetic diversity, history of cross-species transmission, ability to cause a range of diseases, and extraordinary immune-evasion capabilities—would pose unique challenges if an arterivirus were to emerge in humans (7, 29). Indeed, there is growing concern that some arteriviruses pose an underrecognized zoonotic threat (19, 30, 31). Without correlates of natural protection (due to infection), current pandemic-preparedness "platform" technologies that rely upon effective anti-viral immune responses (i.e., vaccines and therapeutic antibodies) are likely to fail against arteriviruses. If an arterivirus were to emerge in humans, the systems, methods, and tools achieved in this study would be vital in the development of effective medical countermeasures. At the very least, the LDV model now seems positioned to advance countermeasures against PRRSV-1/2, which is a significant and ongoing threat to the global swine industry.

Finally, the discovery of mCD163 as the likely receptor for LDV will also enable studies to dissect the molecular barriers to arterivirus cross-species transmission, providing an evidence-based zoonotic risk assessment for viruses in this family. With the tools and methods described herein, isolation and mechanistic studies of additional rodent arteriviruses—thus far only identified via metagenomic surveys—are now readily achievable. More specifically, CD163 appears to be a key molecular determinant of arterivirus species and tissue tropism (18, 31). Our finding that LDV can efficiently infect grivet MA-104 cells complemented with mCD163 extends this idea, suggesting that, at least in some scenarios, CD163 compatibility may be the sole determinant of arterivirus spillover into new hosts. Considering the growing evidence for CD163 utilization as a generalizable feature of arterivirus infection (with the notable exception of EAV), ectopic expression of CD163 orthologs from natural hosts may enable the isolation (and/or rescue of molecular clones) of previously non-cultivable arteriviruses.

MATERIALS AND METHODS

Virus nomenclature

Historically, abbreviations for LDV strains have been somewhat inconsistently applied. For example, the Plagemann strain has been abbreviated as LDV-P, LDV_P, and LDVp, with LDV_P used most frequently. This contrasts with the hyphenated abbreviation for LDV-C. To generate consistency across strains within this paper, we have opted to identify each strain by a lowercase letter immediately following "LDV" (e.g., LDVp, LDVc, and LDVw).

Viruses

Material containing LDVp and LDVw was provided for these studies by K.F. LDVw was isolated from a wild rodent in 1994–1995 by K.F. and Peter Plagemann; no other metadata on this isolate is currently available. Material containing LDVc was provided by M.B. To generate LDV stocks, wild-type C57BL/6J laboratory mice (3–6 weeks of age) obtained from Jackson Laboratories (via the Mouse Breeding Core at the University of Wisconsin–Madison, Madison, WI, USA) were inoculated intraperitoneally with ≈50 µL of source material and euthanized via CO_2 asphyxiation at 24 h post-inoculation, at which time maximal blood draws were performed. Purified sera were diluted in PBS + 2% heat-inactivated fetal calf serum (FCS, Omega Scientific, Tarzana, CA, USA) and frozen in 300-µL aliquots at −80°C.

Cell lines

House mouse (*Mus musculus* Linnaeus, 1758) RAW 264.7 macrophages, laboratory mouse BV-2 microglia, laboratory mouse NIH/3T3 fibroblasts, and house mouse LADMAC monocyte macrophages were obtained from Michael Diamond (Washington University in St. Louis, MI, USA). Embryonic grivet [*Chlorocebus aethiops* (Linnaeus, 1758)] MA-104 kidney cells were obtained from Megan Baldridge (Washington University in St. Louis). House mouse J774A.1 macrophages were obtained from the American Type Culture Collection (ATCC, Manassas, VA, USA). Laboratory mouse ImKC Kupffer cells were obtained from Millipore-Sigma. All cells were maintained according to recommendations by ATCC and/or the manufacturers, including monthly testing for mycoplasma contamination (none identified). Optimal concentrations of puromycin, blasticidin, and hygromycin (Gibco, Billings, MT, USA) were empirically determined for each vector × cell line combination. Photographs of cells were obtained on a Rebel microscope (Echo, San Diego, CA, USA).

In vitro LDV growth kinetics

Virus was added to adherent cell cultures at the appropriate MOI when cells were ≈70–90% confluent, in the minimal amount of media (2% FCS) required to cover the cells. Cultures were incubated at 37°C for 1 h, with rocking every 15 min, followed by removal of inocula and three washes with PBS. Cell-specific media (per ATCC recommendation) were then added to wells and collected at specified time points for storage at −80°C until titration by RT-qPCR or plaque assay.

LDV plaque assay

Tenfold serial dilutions of each sample were made in Dulbecco's modified eagle's medium + 2% FCS (Gibco, Omega Scientific), and 400 µL of each dilution was added to confluent monolayers of cells in a 24-well plate (TPP, Trasadingen, CHE). Assay plates were incubated at 37°C for 1 h, with rocking every 15 min, followed by an overlay of 400 µL of 2% methylcellulose (Sigma-Aldrich, St. Louis, MO, USA) + 2× minimum essential medium (Gibco) + 1% FCS. Optimal plaques were visualized at 3 d post-inoculation by fixing cells for 30 min with 4% paraformaldehyde (PFA) in PBS then staining with 0.05% crystal violet (Sigma-Aldrich) in methanol. Plaque counts were tabulated manually.

Ectopic expression of host genes

Initial mCD163 *trans*-complementation experiments utilized the pLHCX retroviral vector (32), pCS2-mGP encoding murine leukemia virus gag-pol (32), and pCMV-VSV-g (Cat#8454; AddGene, Watertown, MA, USA), as described in Warren et al. (31); later experiments utilized the Sleeping Beauty transposase system (33). All pSBbi vectors were obtained from AddGene. mCD163 was RT-PCR amplified from murine peritoneal macrophages using primers containing homology arms for Gibson assembly (in parentheses in primers, below) into pSBbi vectors cut with *Sfi*I (New England Biolabs, Ipswich, MA, USA):

Forward primer: 5′-
GTGTCGTGAAAACTACCCCAAGCTGGCCTCTGAGGCC)ACGGAGCCATCAAAATCAT
C-3′; reverse primer: 5′-
AGAGAATTGATCCCCAAGCTTGGCCTGACAGGCC)GCCATCTCCAGGGCTATACA-3′.

Collection of murine peritoneal cells

Mice were euthanized via CO_2 asphyxiation in compliance with approved University of Wisconsin–Madison Institutional Animal Care and Use Committee procedures. Following euthanasia, overlying skin was carefully removed from the peritoneum, and 5 mL of ice cold Roswell Park Memorial Institute medium (RPMI; Gibco) supplemented with 10% fetal bovine serum (FBS; Omega Scientific), 1% 4-(2-hydroxyethyl)-1-piperazineethanesulfonic acid (HEPES; Gibco), 1% sodium pyruvate (Gibco), 1% L-glutamine, and 1% antibiotic/antimycotic (Gibco) was injected into the peritoneal cavity using a 5-mL syringe and 25 g needle. Once filled, a curved hemostat was used to clamp the injection site, and the cavity was manually agitated for 2 min. Liquid was recovered using a 25 g needle and a 5-mL syringe and then placed into a 15-mL conical tube on ice. Cells were recovered by centrifugation at 500 × *g* for 5 min and then plated for experiments in RPMI + 10% FBS + 1% HEPES + 1% sodium pyruvate + 50 µg/mL gentamicin (Gibco).

RNA extraction

RNA was extracted from sera or cells using the KingFisher Flex (Thermo Fisher Scientific, Waltham, MA, USA) with MagMax reagents. Carrier RNA was omitted for cellular samples and those destined for sequence-independent single-primer amplification (SISPA) sequencing but included when RNA was extracted from serum.

Virus sequencing and informatics

cDNA was generated from extracted RNA using a revised SISPA approach. First, 30 µL of extracted total nucleic acids was treated with TURBO DNase (Thermo Fisher Scientific) and concentrated to 10 µL with an RNA Clean & Concentrator-5 kit (Zymo Research, Irvine, CA, USA). Next, 1 µL of Primer A [40 pmol/µL; 5′-GTT TCC CAC TGG AGG ATA-(N9)-3′] was added to 4 µL of concentrated viral RNA and heated in a thermocycler at 65°C for 5 min and cooled at 4°C for 5 min. Reverse transcription was performed by adding 5 µL of Superscript IV (SSIV) reverse transcription master mix containing 1 µL of deoxyribonucleotide triphosphate (dNTP; 10 mM), 0.5 µL of dithiothreitol (0.1 M), 1 µL of PCR water, 2 µL of 5× RT buffer, and 0.5 µL of SSIV RT to the reaction mix. The mix was incubated in a thermocycler at 42°C for 10 min. Second-strand cDNA synthesis was performed by adding 5 µL of Sequenase reaction mix (3.85 µL of PCR water, 1 µL of 5× Sequenase reaction buffer, and 0.15 µL of Sequence enzyme) to the reaction mix and incubating at 37°C for 8 min. After incubation, 0.45 µL of the Sequenase dilution buffer and 0.15 µL of Sequenase were added to the reaction mix and incubated at 37°C for 8 min. To amplify the cDNA, 5 µL of the cDNA was added to 45 µL of the Primer B reaction mix containing 0.5 µL of AccuTaq LA DNA polymerase, 5 µL of AccuTaq LA 10× buffer, 1 µL of Primer B (100 pmol/µL; 5′-GTT TCC CAC TGG AGG ATA-3′), 2.5 µL of dNTP (10 mM), 1 µL of dimethyl sulfoxide, and 35 µL of PCR water. The cDNA was amplified using the following thermocycler conditions: 98°C for 30 s, 30 cycles (94°C for 15 s, 50°C for 20 s, and 68°C for 2 min), and 68°C for 10 min. After the incubation, the amplified PCR product was purified using AMPure XP beads (Beckman Coulter, Brea, CA, USA) at a 1:1 concentration and eluted in 50 µL of PCR water. The purified PCR products were quantified with the Qubit dsDNA high-sensitivity kit (Invitrogen, Waltham, MA, USA). SISPA-prepared cDNA material was submitted to the University of Wisconsin–Madison Biotechnology Center. Samples were prepared according to the QIAGEN FX DNA Library Preparation Kit (QIAGEN, Germantown, MD, USA). The quality and quantity of the finished libraries were assessed using a Tapestation (Agilent, Santa Clara, CA, USA) and a Qubit dsDNA HS Assay Kit, respectively. Paired-end 150-bp sequencing was performed using

the NovaSeq6000 system (Illumina, San Diego, CA, USA). Coding-complete genome sequences were assembled from raw sequencing reads using *de novo* assembly and iterative mapping in Geneious Prime 2022.1.1. Annotations were then transferred from the previously published and annotated LDVp sequence (RefSeq #NC_001639) to newly obtained consensus sequences via a MUSCLE alignment. GenBank accession numbers for the viruses sequenced in this study are LDVc, OQ570965; LDVp, OQ570966; and LDVw, OQ570967. Percent-amino-acid identity plots were generated from MUSCLE alignments of translated proteins, with identity for each pairwise comparison calculated along a sliding window of seven amino acids and a step size of 1. This calculation and visualizations of the results are implemented in a Jupyter Notebook, available in Dryad.

Quantification of virus by RT-qPCR

A primer/probe set specific for the *N* gene of LDV was designed using Primer3 (v. 0.4.0): F-5′-TGACTCCGGAGGGATCAAT-3′; R-5′-GCATTAATTAGCCGAACAGTGG-3′; P-5′-/56-FAM/TCAGTTTCATGCTTCCAACG/3BHQ_1/-3′. An RNA standard was made by cloning a flanking segment of the LDV *N* ORF sequence into the pJET1.2/blunt vector (Invitrogen). After linearization of the construct, transcription was performed *in vitro* for 6 h with the MEGAscript T7 transcription kit (Invitrogen), followed by purification using the MEGAclear transcription cleanup kit (Invitrogen), quantification, and dilution to a concentration of 1×10^{10} transcript copies per microliter. Tenfold dilutions of this transcript were used as a standard curve, which was linear over 8 orders of magnitude and sensitive down to 10 copies of RNA transcript per reaction.

Viral RNA was extracted on the KingFisher Flex System (ThermoFisher) using the MagMAX Viral RNA kit. RNA was reverse transcribed and amplified using the TaqMan RNA-to-CT 1-Step Kit (ThermoFisher) on a QuantStudio 6 Pro Real-Time PCR instrument (Applied Biosystems, Waltham, MA, USA). Reverse transcription was performed at 48°C for 15 min followed by 2 min at 95°C. Amplification was accomplished over 50 cycles as follows: 95°C for 15 s and 60°C for 1 min. The reaction mixture contained final concentrations of primers and probes of 500 and 100 nM, respectively.

Quantification of host genes by RT-qPCR

Primer/probe assays were ordered from IDT (Newark, NJ, USA). mCD163 forward primer: 5′-GTCCTCCTCATTGTCTTCCTC-3′; reverse primer: 5′-ATCCGCCTTTGAATCCATCTC-3′; probe: 5′–56-FAM/AGTCGCTGA/ZEN/ATCTGTCGTCGCTTC/3IABkFQ-3′; actin beta forward primer: 5′-GATTACTGCTCTGGCTCCTAG-3′; reverse primer: 5′-GACTCATCGTACTCCTGCTTG-3′; probe: 5′-CTGGCCTCACTGTCCACCTTCC-3′. RNA extraction was performed on 2.5×10^5 to 1×10^6 cells, and RT-qPCR conditions were identical to those described above. Relative abundance of RNA was determined using 2-ΔCt with actin beta as the housekeeping gene followed by 2-ΔCt $\log_{10}$ transformation.

CD163-knockout mice

Cryopreserved spermatocytes were obtained from MMRRC Stock # 046981-UCD (official name: C57BL/6N-Cd163$^{tm1.1(KOMP)Vlcg}$/Mmucd), and *in vitro* fertilization was performed by the UW–Madison Animal Models Core using wild-type C57BL6/J females. mCD163 knockout was confirmed using a custom genotyping assay (Transnetyx, Cordova, TN, USA). F1 heterozygous *mCD163*$^{+/-}$ were mated to generate homozygous *mCD163*$^{-/-}$ (i.e., knockout) mice, which were then maintained in the UW–Madison Mouse Breeding Core by breeding homozygous males and homozygous females.

Mouse exposure experiments

C57BL/6J mice 3–6 weeks of age of both sexes were inoculated by instilling 50 µL of virus inoculum into the peritoneal cavity. Blood was collected via the cheek-bleed method

using a sterile lancet and serum-separator microtainers (BD Lifesciences, Franklin Lakes, NJ, USA).

In situ hybridization

Tissues were placed in 10% neutral-buffered formalin immediately upon harvest and allowed to fix for 3 d. Tissues were embedded in paraffin, and slices were mounted on glass slides. LDV RNA was visualized by *in situ* hybridization using a custom LDV probe targeting the *N* ORF and the RNAscope 2.0 HD detection kit (Advanced Cell Diagnostics, Newark, CA, USA) according to the manufacturer's instructions with Gill's hematoxylin counterstain.

Quantification of CD163 expression by flow cytometry

Adherent cells were detached with CellStripper (Corning, Corning, NY, USA) and transferred to a 96-well V-bottom plate (Corning). Cells were pelleted by centrifugation at 500 × *g* for 5 min to and washed with PBS (Gibco). Cell pellets were then stained with Zombie Violet fixable viability stain (Biolegend, San Diego, CA, USA) for 20 min in the dark. Cell pellets were either fixed/permeabilized using FoxP3 buffer kit (Invitrogen) and then stained for intracellular antigen or surface stained prior to fixation.

For fixing/permeabilization, cells were fixed in 1X buffer for 20 min in the dark. Cells were washed with a diluted 1X permeabilizing buffer with 1 mM ethylenediamine tetraacetic acid (EDTA). Non-specific Fc receptor binding to antibodies was blocked using mouse TruStain FcX (Biolegend), in 1X permeabilizing buffer + EDTA, according to the manufacturer's instructions. Cells were resuspended in 1X permeabilizing buffer + EDTA with a monoclonal anti-mCD163 antibody (Invitrogen, Clone TNKUPJ, PerCP-eFluor 710) or an anti-rat immunoglobulin G 2 (IgG2) kappa isotype control antibody (Invitrogen, PerCP-eFluor 710) at the manufacturer's recommended concentration. Cells were washed and kept in the 1X permeabilizing buffer +EDTA until running on the cytometer.

For staining/fixing, Fc receptor binding to antibodies was blocked using mouse TruStain FcX as done for fix/buffer samples, but in fluorescence-activated cell-sorting (FACS) buffer (PBS + 1 mM EDTA + 2% FCS). Cells were resuspended in FACS buffer with the anti-mCD163 antibody or anti-rat isotype control antibody at manufacturer's recommended concentration. Cells were fixed in 4% PFA for 20 min, then washed with, and stored in FACS buffer until analysis. Cell samples were filtered using 100-µm nylon mesh prior to running on a Northern Lights full-spectrum flow cytometer (Cytek Biosciences, Bethesda, MD, USA). Amine Reactive Compensation beads (Invitrogen), UltraComp beads (Invitrogen), and unstained controls were used for establishing gates. Results were analyzed using FlowJo v10.8 software (BD Life Sciences).

Phylogenetic analysis

Arterivirus sequences were obtained from NCBI or, for the LDV strains used in this study, deep sequenced. Multiple sequence alignments were generated using MUSCLE in Geneious software with default parameters. Phylogenetic relationships were inferred using the maximum-likelihood method based on the Tamura-Nei model (34). The tree with the highest log likelihood (−102949.92) is shown in Fig. 3. Initial tree(s) for the heuristic search were obtained automatically by applying the Neighbor-Join and BioNJ algorithms to a matrix of pairwise distances, estimated using the Tamura-Nei model, and then selecting the topology with superior log likelihood value. The tree was drawn to scale, with branch lengths measured in the number of substitutions per site. Bootstrap analysis was used to test the robustness of the tree topology (1,000 resamplings). Evolutionary analyses were conducted in MEGA 11 (35, 36).

ACKNOWLEDGMENTS

We thank the Genome Editing and Animal Models Shared Resource, the Biomedical Research Model Services Breeding Core, and the Research Animals Resources and

Compliance staff at the University of Wisconsin–Madison. We also thank the University of Wisconsin Biotechnology Center DNA Sequencing Facility (Research Resource Identifier – RRID: SCR_017759) for providing NovaSeq6000 sequencing services. Additionally, we thank Anya Crane (National Institutes of Health [NIH] National Institute of Allergy and Infectious Diseases [NIAID] Integrated Research Facility at Fort Detrick [IRF-Frederick]) for critically editing the manuscript.

The authors thank the Office of the Vice Chancellor for Research and Graduate Education, the School of Medicine & Public Health, and the Department of Pathology & Laboratory Medicine at the University of Wisconsin–Madison for startup funding (allocated to A.L.B.). This work was funded in part by the NIH (grant no. K99-AI151256-01A1 to C.J.W.). This work was supported by the NIAID of the NIH (grant no. T32AI55397 to M.D.R.) and by the National Institute of General Medical Sciences of the NIH (grant no. T32GM135119 to S.M.M.). This work was also supported in part through Laulima Government Solutions, LLC, prime contract with the NIH NIAID, under contract no. HHSN272201800013C. J.H.K. performed this work as an employee of Tunnell Government Services (TGS), a subcontractor of Laulima Government Solutions, LLC, under contract no. HHSN272201800013C.

The views and conclusions contained in this document are those of the authors and should not be interpreted as necessarily representing the official policies, either expressed or implied, of the U.S. Department of Health and Human Services or of the institutions and companies affiliated with the authors, nor does mention of trade names, commercial products, or organizations imply endorsement by the U.S. Government.

The authors declare no competing interests.

AUTHOR AFFILIATIONS

[1]Department of Pathology and Laboratory Medicine, University of Wisconsin–Madison School of Medicine and Public Health, Madison, Wisconsin, USA
[2]Department of Biology, Georgia State University, Atlanta, Georgia, USA
[3]Virus and Prion Research Unit, USA Department of Agriculture, National Animal Disease Center, Ames, Iowa, USA
[4]Integrated Research Facility at Fort Detrick, Division of Clinical Research, National Institute of Allergy and Infectious Diseases, National Institutes of Health, Fort Detrick, Frederick, Maryland, USA
[5]Department of Veterinary Biosciences, The Ohio State University, Columbus, Ohio, USA

AUTHOR ORCIDs

Jens H. Kuhn http://orcid.org/0000-0002-7800-6045
Adam L. Bailey http://orcid.org/0000-0002-6560-9680

FUNDING

Funder	Grant(s)	Author(s)
HHS | National Institutes of Health (NIH)	K99-AI151256-01A1	Cody J. Warren
HHS | NIH | National Institute of Allergy and Infectious Diseases (NIAID)	T32AI55397	Mitchell D. Ramuta
HHS | NIH | National Institute of General Medical Sciences (NIGMS)	T32GM135119	Sara M. Maloney
HHS | NIH | National Institute of Allergy and Infectious Diseases (NIAID)	HHSN272201800013C	Jens H. Kuhn

AUTHOR CONTRIBUTIONS

Teressa M. Shaw, Conceptualization, Data curation, Formal analysis, Writing – review and editing | Sara M. Maloney, Data curation, Formal analysis, Writing – review and editing | Kylie Nennig, Data curation, Formal analysis, Writing – review and editing | Mitchell D.

Ramuta, Data curation, Formal analysis, Writing – review and editing | Andrew Norton, Data curation, Writing – review and editing | Rodrigo Ibarra, Data curation, Writing – review and editing | Paul Kuehnert, Data curation, Writing – review and editing | Kay Faaberg, Resources, Writing – review and editing | Jens H. Kuhn, Conceptualization, Writing – review and editing | David H. O'Connor, Formal analysis, Resources, software, Writing – review and editing | Cody J. Warren, Conceptualization, Data curation, Formal analysis, Writing – review and editing | Adam L. Bailey, Conceptualization, Data curation, Formal analysis, Funding acquisition, Investigation, Methodology, Project administration, Resources, Supervision, Visualization, Writing – original draft, Writing – review and editing.

DATA AVAILABILITY

Raw data sets used to make each figure have been uploaded to Dryad and associated with Adam Bailey's ORCiD: 0000–0002-6560-9680.

ETHICS APPROVAL

All experiments were conducted by trained personnel and in compliance with NIH and UW–Madison policies and procedures (Institutional Animal Care and Use Committee: M006443; Institutional Biosafety Committee: B00000929).

ADDITIONAL FILES

The following material is available online.

Supplemental Material

Fig. S1 (JVI00930-23-s0001.pdf). Flow cytometry data.
Fig. S2 (JVI00930-23-s0002.pdf). LDV CPE on NIH 3T3.
Fig. S3 (JVI00930-23-s0003.pdf). Flow Cytometry for MA104.
Fig. S4 (JVI00930-23-s0004.tif). MA104+EV inoculated with LDV.
Fig. S5 (JVI00930-23-s0005.pdf). Flow cytometry.

REFERENCES

1. Snijder EJ, Kikkert M, Fang Y. 2013. Arterivirus molecular biology and pathogenesis. J Gen Virol 94:2141–2163. https://doi.org/10.1099/vir.0.056341-0
2. Howley PM, Knipe DM. 2023. RNA viruses. 7th ed. Wolters Kluwer, Philadelphia.
3. Shi M, Lin X-D, Chen X, Tian J-H, Chen L-J, Li K, Wang W, Eden J-S, Shen J-J, Liu L, Holmes EC, Zhang Y-Z. 2018. The evolutionary history of vertebrate RNA viruses. Nature 561:197–202. https://doi.org/10.1038/s41586-018-0310-0
4. Kuhn JH, Lauck M, Bailey AL, Shchetinin AM, Vishnevskaya TV, Bào Y, Ng TFF, LeBreton M, Schneider BS, Gillis A, Tamoufe U, Diffo JLD, Takuo JM, Kondov NO, Coffey LL, Wolfe ND, Delwart E, Clawson AN, Postnikova E, Bollinger L, Lackemeyer MG, Radoshitzky SR, Palacios G, Wada J, Shevtsova ZV, Jahrling PB, Lapin BA, Deriabin PG, Dunowska M, Alkhovsky SV, Rogers J, Friedrich TC, O'Connor DH, Goldberg TL. 2016. Reorganization and expansion of the *Nidoviral* family *Arteriviridae*. Arch Virol 161:755–768. https://doi.org/10.1007/s00705-015-2672-z
5. Bailey AL, Lauck M, Ghai RR, Nelson CW, Heimbruch K, Hughes AL, Goldberg TL, Kuhn JH, Jasinska AJ, Freimer NB, Apetrei C, O'Connor DH, Silvestri G. 2016. Pegiviruses, and lentiviruses are common among wild African monkeys. J Virol 90:6724–6737. https://doi.org/10.1128/JVI.00573-16
6. Riley V, Lilly F, Huerto E, Bardell D. 1960. Transmissible agent associated with 26 types of experimental mouse neoplasms. Science 132:545–547. https://doi.org/10.1126/science.132.3426.545
7. Plagemann PG, Rowland RR, Even C, Faaberg KS. 1995. Lactate dehydrogenase-elevating virus: an ideal persistent virus? Springer Semin Immunopathol 17:167–186. https://doi.org/10.1007/BF00196164
8. van den Broek MF, Spörri R, Even C, Plagemann PG, Hänseler E, Hengartner H, Zinkernagel RM. 1997. Lactate dehydrogenase-elevating virus (LDV): lifelong coexistence of virus and LDV-specific immunity. J Immunol 159:1585–1588. https://doi.org/10.1016/S0165--2478(97)86210-4
9. Anderson GW, Rowland RR, Palmer GA, Even C, Plagemann PG. 1995. Lactate dehydrogenase-elevating virus replication persists in liver, spleen, lymph node, and testis tissues and results in accumulation of viral RNA in germinal centers, concomitant with polyclonal activation of B cells. J Virol 69:5177–5185. https://doi.org/10.1128/JVI.69.8.5177-5185.1995
10. Inada T, Mims CA. 1985. Pattern of infection and selective loss of Ia positive cells in suckling and adult mice Inoculated with lactic dehydrogenase virus. Arch Virol 86:151–165. https://doi.org/10.1007/BF01309821
11. Kowalchyk K, Plagemann PG. 1985. Cell surface receptors for lactate dehydrogenase-elevating virus on subpopulation of macrophages. Virus Res 2:211–229. https://doi.org/10.1016/0168-1702(85)90010-3
12. Schlesinger S, Lagwinska E, Stewart CC, Croce CM. 1976. Lactic dehydrogenase virus replicates in somatic cell hybrids of mouse peritoneal macrophages and SV40-transformed human fibroblasts. Virology 74:535–539. https://doi.org/10.1016/0042-6822(76)90359-7
13. Inada T. 1993. Replication of lactate dehydrogenase-elevating virus in various species cell lines infected with dual-, ampho- and xenotropic murine leukaemia viruses *in vitro*. Virus Res. 27:267–281. https://doi.org/10.1016/0168-1702(93)90038-o
14. Inada T, Yamazaki S. 1991. Replication of lactate dehydrogenase-elevating virus in cells infected with murine leukaemia viruses *in vitro*. J

Gen Virol 72 (Pt 10):2437–2444. https://doi.org/10.1099/0022-1317-72-10-2437
15. Dokland T. 2010. The structural biology of PRRSV. Virus Res. 154:86–97. https://doi.org/10.1016/j.virusres.2010.07.029
16. Su C-M, Rowland RRR, Yoo D. 2021. Recent advances in PRRS virus receptors and the targeting of receptor-ligand for control. Vaccines (Basel) 9:354. https://doi.org/10.3390/vaccines9040354
17. Calvert JG, Slade DE, Shields SL, Jolie R, Mannan RM, Ankenbauer RG, Welch S-KW. 2007. CD163 expression confers susceptibility to porcine reproductive and respiratory syndrome viruses. J Virol 81:7371–7379. https://doi.org/10.1128/JVI.00513-07
18. Burkard C, Lillico SG, Reid E, Jackson B, Mileham AJ, Ait-Ali T, Whitelaw CBA, Archibald AL. 2017. Precision engineering for PRRSV resistance in pigs: macrophages from genome edited pigs lacking CD163 SRCR5 domain are fully resistant to both PRRSV genotypes while maintaining biological function. PLoS Pathog 13:e1006206. https://doi.org/10.1371/journal.ppat.1006206
19. Boys IN, Elde NC. 2022. When viruses do not go gentle into that good night. Cell Host Microbe 30:1499–1500. https://doi.org/10.1016/j.chom.2022.10.008
20. Stueckemann JA, Holth M, Swart WJ, Kowalchyk K, Smith MS, Wolstenholme AJ, Cafruny WA, Plagemann PGW. 1982. Replication of lactate dehydrogenase-elevating virus in macrophages: 2 mechanism of persistent infection in mice and cell culture. J Gen Virol 59:263–272. https://doi.org/10.1099/0022-1317-59-2-263
21. Plagemann PG. 2001. Complexity of the single linear neutralization epitope of the mouse arterivirus lactate dehydrogenase-elevating virus. Virology 290:11–20. https://doi.org/10.1006/viro.2001.1139
22. Cafruny WA, Jones QA, Haven TR, Zitterkopf NL, Plagemann PGW, Rowland RR. 2003. Glucocorticoid regulation of lactate dehydrogenase-elevating virus replication in macrophages. Virus Res 92:83–87. https://doi.org/10.1016/s0168-1702(02)00321-0
23. Martinez D, Brinton MA, Tachovsky TG, Phelps AH. 1980. Identification of lactate dehydrogenase-elevating virus as the etiological agent of genetically restricted, age-dependent polioencephalomyelitis of mice. Infect Immun 27:979–987. https://doi.org/10.1128/iai.27.3.979-987.1980
24. Godeny EK, Chen L, Kumar SN, Methven SL, Koonin EV, Brinton MA. 1993. Complete genomic sequence and phylogenetic analysis of the lactate dehydrogenase-elevating virus (LDV). Virology 194:585–596. https://doi.org/10.1006/viro.1993.1298
25. Chen Z, Li K, Plagemann PG. 2000. Neuropathogenicity and sensitivity to antibody neutralization of lactate dehydrogenase-elevating virus are determined by polylactosaminoglycan chains on the primary envelope glycoprotein. Virology 266:88–98. https://doi.org/10.1006/viro.1999.0050
26. Palmer GA, Kuo L, Chen Z, Faaberg KS, Plagemann PG. 1995. Sequence of the genome of lactate dehydrogenase-elevating virus: heterogenicity between strains P and C. Virology 209:637–642. https://doi.org/10.1006/viro.1995.1296
27. Green H, Kehinde O. 1976. Spontaneous heritable changes leading to increased adipose conversion in 3T3 cells. Cell 7:105–113. https://doi.org/10.1016/0092-8674(76)90260-9
28. Woolhouse M, Scott F, Hudson Z, Howey R, Chase-Topping M. 2012. Human viruses: discovery and emergence. Philos Trans R Soc Lond B Biol Sci 367:2864–2871. https://doi.org/10.1098/rstb.2011.0354
29. Bailey AL, Lauck M, Sibley SD, Friedrich TC, Kuhn JH, Freimer NB, Jasinska AJ, Phillips-Conroy JE, Jolly CJ, Marx PA, Apetrei C, Rogers J, Goldberg TL, O'Connor DH, Pierson TC. 2016. Zoonotic potential of simian arteriviruses. J Virol 90:630–635. https://doi.org/10.1128/JVI.01433-15
30. Graham BS, Sullivan NJ. 2018. Emerging viral diseases from a vaccinology perspective: preparing for the next pandemic. Nat Immunol 19:20–28. https://doi.org/10.1038/s41590-017-0007-9
31. Warren CJ, Yu S, Peters DK, Barbachano-Guerrero A, Yang Q, Burris BL, Worwa G, Huang I-C, Wilkerson GK, Goldberg TL, Kuhn JH, Sawyer SL. 2022. Primate hemorrhagic fever-causing arteriviruses are poised for spillover to humans. Cell 185:3980–3991. https://doi.org/10.1016/j.cell.2022.09.022
32. Yamashita M, Emerman M. 2004. Capsid is a dominant determinant of retrovirus infectivity in nondividing cells. J Virol 78:5670–5678. https://doi.org/10.1128/JVI.78.11.5670-5678.2004
33. Kowarz E, Löscher D, Marschalek R. 2015. Optimized sleeping beauty transposons rapidly generate stable transgenic cell lines. Biotechnol J 10:647–653. https://doi.org/10.1002/biot.201400821
34. Tamura K, Nei M. 1993. Estimation of the number of nucleotide substitutions in the control region of mitochondrial DNA in humans and chimpanzees. Mol Biol Evol 10:512–526. https://doi.org/10.1093/oxfordjournals.molbev.a040023
35. Stecher G, Tamura K, Kumar S. 2020. Molecular evolutionary genetics analysis (MEGA) for macOS. Mol Biol Evol 37:1237–1239. https://doi.org/10.1093/molbev/msz312
36. Tamura K, Stecher G, Kumar S. 2021. Mega11: molecular evolutionary genetics analysis version 11. Mol Biol Evol 38:3022–3027. https://doi.org/10.1093/molbev/msab120